Results in Engineering 18 (2023) 101042

Contents lists available at ScienceDirect

Results in Engineering

journal homepage: www.sciencedirect.com/journal/results-in-engineering

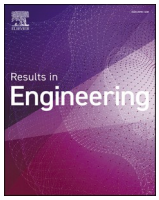

Design of partial height web stiffeners in beam-to-column joints and influence of residual stresses induced by welding

B. Kövesdi [a,*], L. Dunai [a], H. Pasternak [b], Z. Li [c], R. Oly [d], P. Márai [d]

[a] Budapest University of Technology and Economics, Faculty of Civil Engineering, Department of Structural Engineering, Műegyetem, rkp. 3, 1111, Budapest, Hungary
[b] Brandenburg University of Technology, Institute of Civil and Structural Engineering, Platz der Deutschen Einheit1, 03046, Cottbus, Germany
[c] Technische Universität Berlin, Institut für Bauingenieurwesen, G.-Meyer-Alle 25, 13355, Berlin, Germany
[d] Astron Buildings s.a., Route d'Ettelbruck, 9230, Diekirch, Luxembourg

ARTICLE INFO

Keywords:
Web panel in shear
Steel frames
Knee joints
Beam-to-column joints
Partial stiffeners

ABSTRACT

Fixed beam-to-column joints in steel portal frames with bolted connections typically present stiffeners to ensure proper load bearing resistance and stiffness to the joint. Executing the same stiffeners with a reduced height (e.g. partial height web stiffener) allows for cost saving during manufacturing but must be paid off by considering its effects in the design verification of the joint. The usual gap size of the partial stiffener has a height of 10%–30% of the concerned element web depth. Based on the Astron product example, this study analyzes the effects of the partial stiffener on the concerned knee joint resistance components according EN1993-1-8. A numerical parametric study is performed based on an advanced 3D FEM model to determine and compare the structural behavior of the beam-to-column joints with full and partial stiffeners. Comparison of the calculation results prove, the partial stiffener influences only the shear panel resistance component, and it has no effect on other components of the joint. The failure mechanism of the shear panel using different slenderness ratios are analyzed in the paper and an enhanced design method is developed, which allow to consider the geometrical gap between the flange and stiffeners. The effect of residual stresses resulting from the manufacturing processes of the plated elements is also analyzed and introduced in the paper using advanced weld simulation technique.

1. Introduction

Portal frames made of welded steel elements typically use fixed end plate beam-to-column joints at their knees to connect the column and the rafter. The web panel of the joint is square or rectangular and contains a web stiffener, which, together with the external flange, the connection plate, and the end plate, forms a frame around the knee web. The typical configuration can be seen in Fig. 1a). During manufacturing of these joints, the stiffener should be placed between the flange and the connection plate. Therefore, its length should be fitted with large accuracy and the manufacturing tolerance should be kept small, which can significantly increase its manufacturing cost. In the case of numerous industrial projects, the manufacturing and welding of these small stiffeners fitted between the two flanges did cause issues during assembly of the column shape. Especially, for those cases, where the flange imperfection reduced the gap between the two flanges after performing the welding seem between the column web and flanges. Therefore, there is an industrial need to investigate the structural behavior and resistance of these joints, if the stiffener length is kept significantly smaller than the web depth, as shown in Fig. 1b). Using these smaller length "partial" stiffeners, the assembly problems could be significantly reduced, however its application requires the detailed investigation of the joint structural behavior. This configuration means, the stiffener is welded only to the connection plate and web of the column, resulting a plate supported along three edges. Another significant difference is that the frame - formed from the flanges, connection plate and stiffeners - partly loses its stiffness and strength due to the gap, which needs a detailed investigated of these joints. So, the gap potentially saves cost due to reduced preparation and welding efforts but might require thicker plates to balance its structural effect. The gap is always located at the outer flange side and can measure from 10% to 30% of the column/beam web depth. This study analyzes the partial stiffener effect on the structural behavior and the resistance calculation method, considering the influence of residual stresses.

The novelty of the current research is within the analysis of the structural behavior and bending resistance of the knee joints using

* Corresponding author.
E-mail address: kovesdi.balazs@emk.bme.hu (B. Kövesdi).

https://doi.org/10.1016/j.rineng.2023.101042
Received 26 January 2023; Received in revised form 17 March 2023; Accepted 18 March 2023
Available online 25 March 2023

partial length web stiffeners. According to the author's knowledge previous studies investigated knee joint behavior with full-length stiffeners or without stiffeners. The application of partial length web stiffener and its design is completely new in the international literature.

The first part of the paper presents a numerical model development and analysis, investigating which components of the EN1993-1-8 [1] component method is affected by the stiffener length. Each component of the component method is investigated on separated models adjusting the joint geometry and force the failure mode happening in the investigated component. Based on the comparison of the joint behavior and resistance with full and partial stiffeners the effect of the gap size is determined, and the mechanical properties and resistance of the components are characterized in terms of the partial stiffener. The numerical results show, only the resistance of the web panel in shear component is influenced by the partial stiffener; all the other component resistances are not affected by the partial stiffener, where the gap size cannot exceed 30% of the web depth.

Therefore, only the shear panel resistance calculation is investigated in the present paper in a detailed manner. The shear panel resistance calculation method is based on the EN1993-1-8 [1] for the bolted connection and the Astron Buildings ETA-18/1027 [2] for the knee joint. The most advanced resistance calculation model contains three basic resistance components, i.e. tension band resistance, shear buckling resistance and frame mechanism (see Fig. 2). These go back to earlier works of Scheer, Pasternak and Schween [3], Vayas, Pasternak and Schween [4] and Vayas, Ermopoulos and Pasternak [5] and Jaspart [21]. From these three components the tension band and the frame mechanism are so called post-critical components, which are activating after buckling of the web panel having large plastic deformations. There is also a fourth possible failure mode of the shear panel, which is the plastic failure, and it can also activate the frame mechanism additionally. Within a numerical parametric study, the influence magnitudes and dependencies of these components are determined, where hundreds of geometrical variations of the beam-to-column joint are analyzed. Results of the entire parametric study is documented in Ref. [6], the current paper contains the main outcomes of the study and conclusions which could help to understand the mechanical behavior of knee joints with partial stiffener.

The second part of the paper introduces a numerical parametric study with the aim to determine the bending resistance of the investigated joints with partial stiffener, to compare the calculated resistances to the joints with full stiffener and to develop enhanced design proposals for the shear panel resistance based on the design method of EN1993-1-8 [1]. The numerical results proved, the structural behavior of the shear panel and the proportion of the above described three components significantly depends on the slenderness of the web and the flange sizes. Therefore, the enhanced design method is developed considering the slenderness of the shear panel and different design equations are proposed for stocky and slender web panel joints corresponding to plastic or elastic buckling failure modes.

The third part of the paper introduces the results of a numerical parametric study highlighting the effect of manufacturing technique and influence of welding induced residual stresses on the shear panel resistance. Plated structures are typically assembled by welding in a certain sequence, starting with the butt welds of the individual web and flange plates (thickness variation), web-flange single sided welds (section assembly), pre-assembling of all other plates (end plates, connection plates, stiffeners, gussets) and final welding. Most welds are executed by welding machines or robots. The Astron fabrication process is used as the example case in the current paper. The models allow to compare the calculated resistances with and without consideration of residual stresses.

2. Numerical model development

Two numerical models are developed using the Finite Element software Ansys 17.1 [7] to investigate the resistance of the beam-to-column joint and the shear panel resistance. The first model shown in Fig. 3a) is a full 3D model using volume elements, the second model is a full shell model as shown in Fig. 3b). The applied finite element is Solid185 in the solid element model, and Shell181 in the shell element model of the Ansys software. The applied solid element is an 8-node volume element having three degrees of freedom at each node, stress stiffening and large deflection capabilities are also included, therefore it fits well for linear and non-linear analysis with large displacements and large strains, and material nonlinearities can be also taken into account. The shell element is a 4-node thin shell element, having 6° of freedom at each node and using Reissner-Mindlin theory. This element is also well suitable for linear and non-linear analysis with large displacements and large strains, and material nonlinearities can be also taken into account. The applied mesh can be seen in Fig. 3 for one specific joint geometry. The accuracy of the mesh is tested and proved by model verification using a mesh sensitivity study. In the numerical model only the beam-to-column joint is modeled with a smaller part of the column and beam shape. The modeled column/beam length is long enough to model the optional failure mode in the beam/column shapes. The bending moment is applied by two uniformly distributed loads acting on the beam flanges. The applied element size is max. 15 mm in the numerical models, which gave a good prediction of the test results in the previous similar investigations done by Kövesdi and Dunai [8].

Bolts and connection plates are considered only in the solid element model using realistic geometries applied in the daily design. The finite element mesh of the bolts and the plates around the bolts are created having only tetrahedral elements, what is a favorable mesh geometry for bolted connections. Contact elements are applied between the connection plate and column flange and between the connection plate and the bolts. The contact elements can work only against compression, and they have no resistance against tension. In the solid element model, the entire

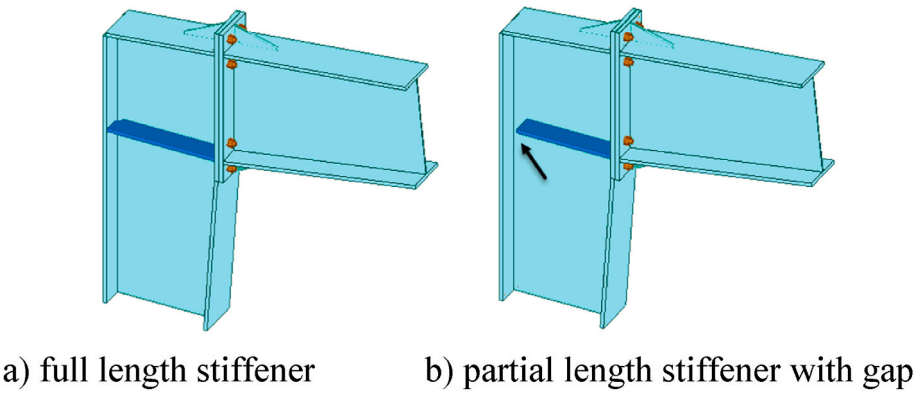

Fig. 1. Typical knee joint with bolted connection and horizontal web stiffener.

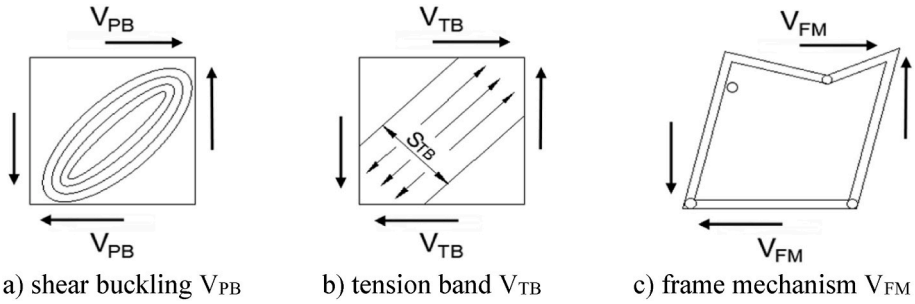

Fig. 2. Main resistance components of the shear panel [21].

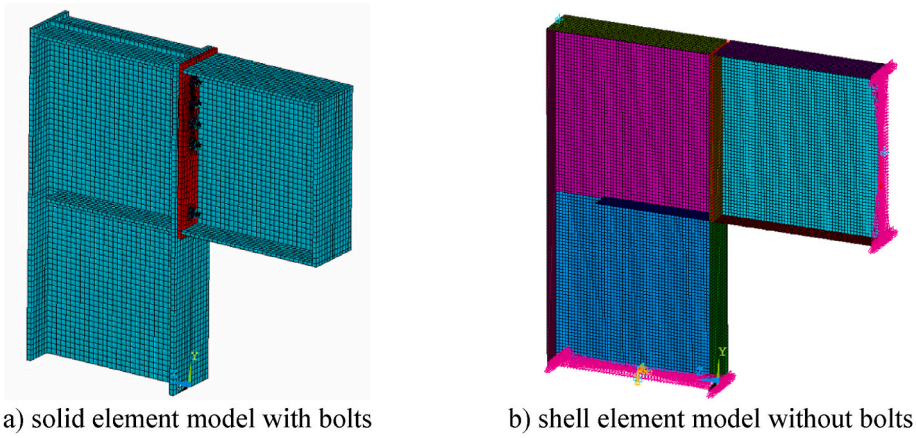

Fig. 3. Applied numerical model of the beam-to-column joint.

beam-to-column joint is modeled with high accuracy capturing the structural behavior and bending resistance accurately.

The ultimate load is determined by geometrically and materially nonlinear analysis with imperfections (GMNIA) using equivalent geometric imperfections in both models. To calculate the ultimate resistance linear elastic - hardening plastic material model is used for the bolts and for the steel plates, too. To model the failure of the bolts and the connection plate the used material model and the applied finite elements must be able to handle large plastic deformations and failure criterion. To ensure these two criteria, volume elements are used which can follow large plastic deformations and multi-linear hardening plastic material model is applied considering damage characteristics in the model. In the material model a multi-linear isotropic hardening rule with the von Mises yield criterion is applied. Degradation of the material model could follow the tensile fracture of the bolts or the plates after a certain elongation. If no degradation would be used in the material model, the plates and bolts could restrain the same resistance by very large deformations, and the numerical calculation could not find the maximum value of the load-displacement curve (load carrying capacity of the joint). This effect would result in a fictive hardening of the joint, what does not exist in the reality. One possible solution for this problem is to model the material degradation. Several research activities are made on this field to determine the degradation function for different steel materials, but since no general solution is given till now, a conservative approach is used in this study by applying linear degradation function.

The applied failure criterion is the definition of softening rules in the multi-linear material model after reaching the failure limit point. According to the material model description in Ref. [7], if a state of stress is found to lay outside of the yield surface a backward-Euler algorithm is used to return the stress to the failure surface. The resulting inelastic increment in strain is then accumulated as crack strain. The maximum stress that can be sustained in an element is then reduced as a function of crack strain. Using this material model the softening slope should be defined by the user. Usually, various unloading paths are driven during the tension tests to be able to detect the damage by decreasing Young's modulus, see e.g. Lemaitre and Dufailly (1987) [9], Bonora et al. (2005) [10], Brünig and Alves (2005) [11] and Celentano and Chaboche (2007) [12]. The effect of the softening slope has been previously investigated in frame of the research program of the hammerhead joints [13] and it was found that in the case of beam-to-column joints it has no effect on the bending resistance. The reason of it is that the maximum reached strain level in the numerical calculations is very near to the failure limit point. After the failure of the first bolt row, all the other bolts in the connection can be rapidly overloaded and fail as well.

Both numerical models (the solid element model and the shell element model) have been validated by comparison of the numerical calculations to test results. Several tests carried out at the Technical University of Braunschweig [5] are re-calculated with the shell element numerical model. This test program was optimal for the model validation, because its research aim was to investigate the web panel in shear resistance of beam-to-column joints with slender web panels. One test made at the Technical University of Braunschweig by Katula [14] is also used in the verification and the resistance of the test specimen is also determined by the numerical model. By all these calculations the same failure mode as in the tests (web panel in shear failure) were observed and a good correlation between the numerical results and the measured resistances is found. The biggest difference obtained is 10%, however, the average difference is smaller than 5%, which is a good fit between the numerical and experimental investigations. The test layout of the experiments carried out at the TU Braunschweig [5] is shown in Fig. 4. The input data of the numerical model (and the measured values of the test specimens regarding the geometry and material properties) are listed in Table 1. The typical failure mode obtained in the numerical model can be seen in Fig. 4b), which is the web panel in shear resistance. The same failure mode has been observed in the executed test program as

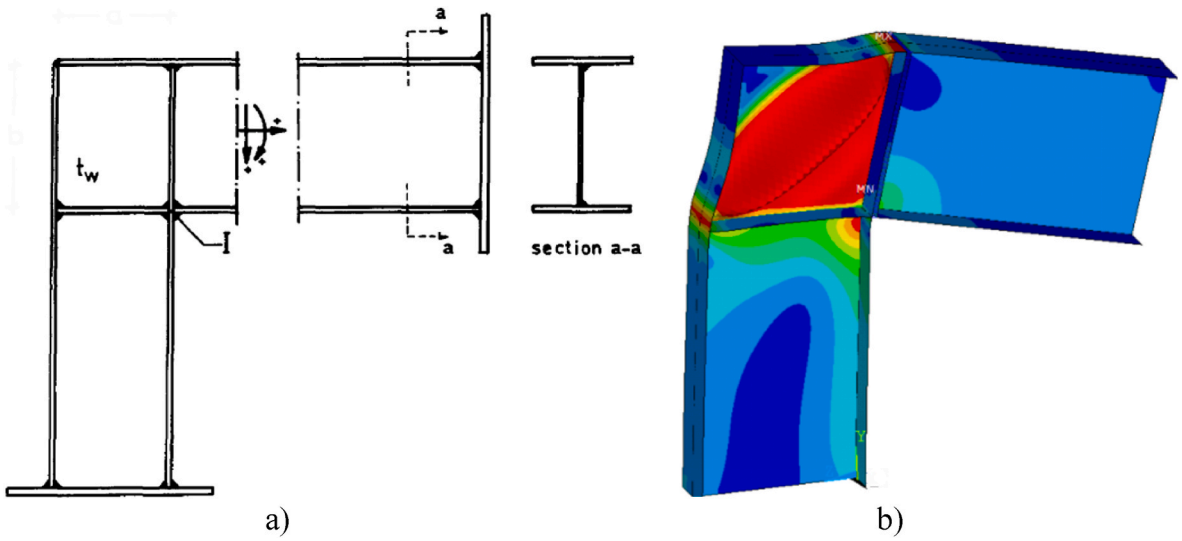

Fig. 4. a) Test layout used for model validation [5], b) typical failure mode obtained by the numerical model.

Table 1
Comparison of the numerical and experimental results on the shear panel resistance.

	Y	h_w	t_w	z	b_1	t_1	b_2	t_2	b_3	t_3	b_4	t_4	f_{yw}	f_{y1}	f_{y2}	f_{y3}	f_{y4}	M_{exp}	M_{num}
	[mm]												[MPa]					[kNm]	
1	200	200	1	200	150	5	150	5	150	5	150	5	230	304	304	304	304	7.8	8.1
2	200	200	1	200	150	9.7	150	9.7	150	9.7	150	9.7	230	278	278	278	278	12.9	13.2
3	240	300	1	300	150	9.7	150	9.7	150	9.7	150	9.7	226	275	275	275	275	17.5	18.4
4	300	240	1	240	150	9.7	150	9.7	150	9.7	150	9.7	226	283	283	283	283	15.4	16.2
5	300	300	2	300	150	5	150	5	150	3	150	3	319	232	232	232	232	24.5	25.07
6	240	300	2	300	150	3	150	3	150	3	150	3	319	232	232	232	232	22.2	24.8
7	240	300	2	300	150	5.2	150	5.2	150	5.2	150	5.2	319	324	324	324	324	24	25.8

Where: Y is the column web depth; h_w is the beam web height; t_w is the shear panel web thickness; b_i and t_i are the plate width and thickness of the four surrounding plates around the web panel in shear; f_{yw} is the yield strength of the web panel; f_{yi} are the yield strength of the surrounding plates.

well.

The solid element model has been also validated to experimental results. The basis of the numerical model development and verification are the experiments carried out at the BME Department of Structural Engineering in 2007 [22]. Three specimens were tested to analyze the structural behavior of connections with hammerhead. The test layout and the analyzed specimen geometry can be seen in Figs. 5 and 6. The cross-section of the analyzed beam had the following dimensions: web depth was equal to 860 mm with the thickness of 8 mm; the flange width was 360 mm with a thickness of 20 mm; the applied bolts in the tests were BSF20 (diameter 20 mm; grade 8.8) in each bolt-rows. The material of the end-plate and the beam was S355. The bolt-row configuration, the bolt size and the material properties of the plates and also the bolts were the same for all the three specimens. The only difference was the

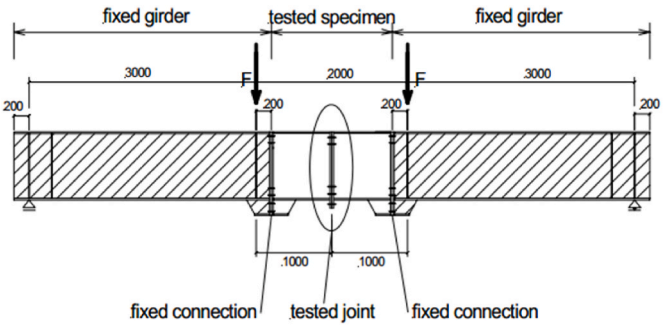

Fig. 5. Test layout used for model verification.

thickness of the end-plate. Specimens with end-plate thickness of 12 mm, 15 mm and 20 mm were tested. The bolt-row positions can be seen in Fig. 6. The analyzed hammerhead had the following dimensions: flange width 360 mm with a thickness of 15 mm; gusset depth 150 mm measured between the upper flange outer side and the hammerhead flange inner side; gusset thickness 8 mm. The length of the hammerhead was 150 mm at the outer side and 250 mm at the inner side, as shown in Fig. 6.

In the verification of the numerical model the observed failure modes, the ultimate moment capacity of the analyzed joints and the bolt-row force distributions at several moment levels are compared. Fig. 7 shows the observed failure mode in the tests and in the numerical analysis. The test and the numerical study showed the same structural behavior. The relevant failure mode in both cases is the combination of yielding in the end-plate and tension failure in the bolts (mode 2).

The calculated deformed shape of the end-plate has also the same character obtained in the tests. The measured and calculated moment capacities are compared for all the three specimens in Table 2.

The results of the numerical model show good agreement with the test results. The observed differences are between 5 and 7%, and all the calculations are on the safe side. It can be explained by the modeling of the material degradation. The end of the linear behavior is also compared, and the results showed the same accuracy as observed in the case of the moment capacities.

The numerical calculations presented in the further numerical parametric study showed the stiffener length has no influence on the tension side component resistances. Therefore, modeling level neglecting the tension side failure can be also applied to determine the component resistances on the compression side. If the determination of

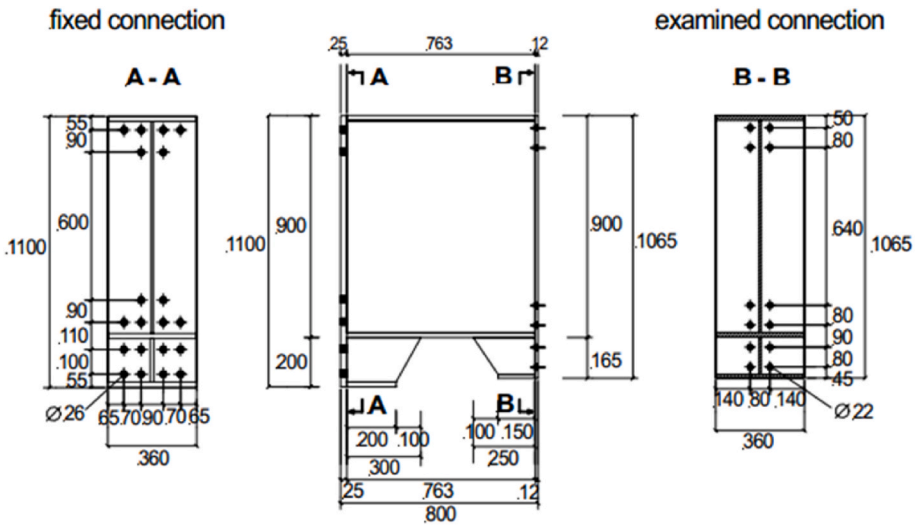

Fig. 6. Geometry of the tested specimen.

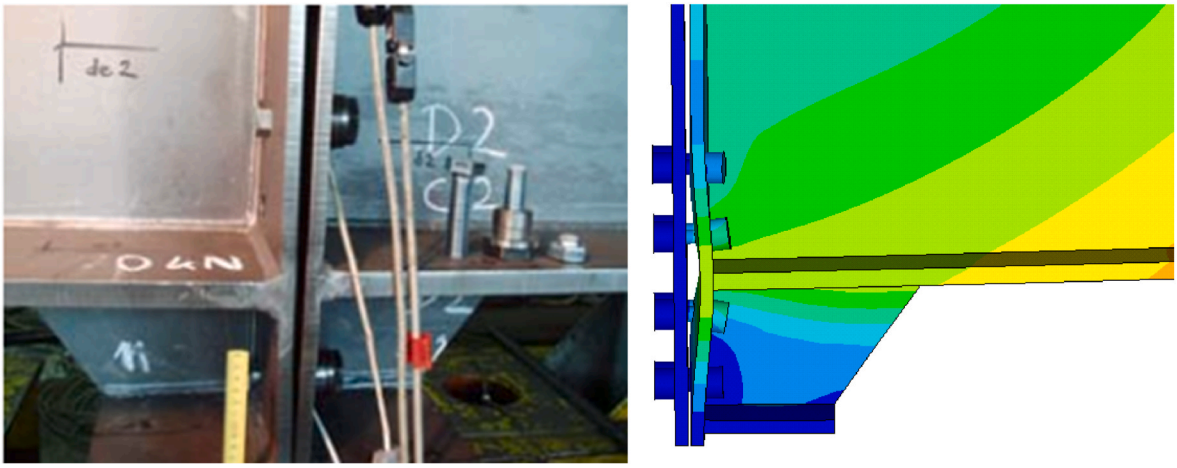

Fig. 7. Comparison of the experimental and numerical failure modes.

Table 2
Comparison of the measured and calculated moment capacities.

specimen	$M_{R,num}$ [kNm]	$M_{R,exp}$ [kNm]	difference [%]
#1	1433	1509	5.1%
#2	1515	1635	7.3%
#3	1490	1608	7.3%

the T-stub and the beam web in tension resistances are not the aim of the further investigations, the modeling of the bolts with volume elements and contact are not necessary, which makes the calculations more time consuming. In this case, using a shell element model, the tension side resistances related to the T-stub failure modes are neglected, but the resistances of all the other components can be determined with the same accuracy as using the solid element model.

Therefore, the solid element model was used to investigate all the components of the joints, and to determine the effect of the partial stiffener on them. These results are presented in Section 3. For the second numerical parametric study, the web panel in shear resistance calculation is made using shell element model. Their results are introduced in Section 4. The effect of the welding is also investigated on a solid element model, which results are presented in Section 5.

3. Numerical parametric study and component influenced by partial stiffener

3.1. Analyzed parameters and structural behavior

The study objects are typical portal frame structures selected from the Astron Building System (ref. ETA-18/1027) product range. There are 6 different components in the joint design of EN1993-1-8 [1] which are relevant for the analyzed beam-to-column joints, and which can be clearly separated by pre-dimensioning of the investigated joint configurations. The general components according to the Eurocode-based design of a beam-to-column joint are shown in Fig. 8 [23]. These components which resistance is investigated in the current research program are the followings:

Components on the tension side:

- *bolts in tension*
  - o *T-stub resistance (mode 1 and 2 – dominant connection plate failure),*
  - o *T-stub resistance (mode 3 – bolt tension failure),*
- *beam web in tension,*
- *column web in tension.*

Components on the compression side:

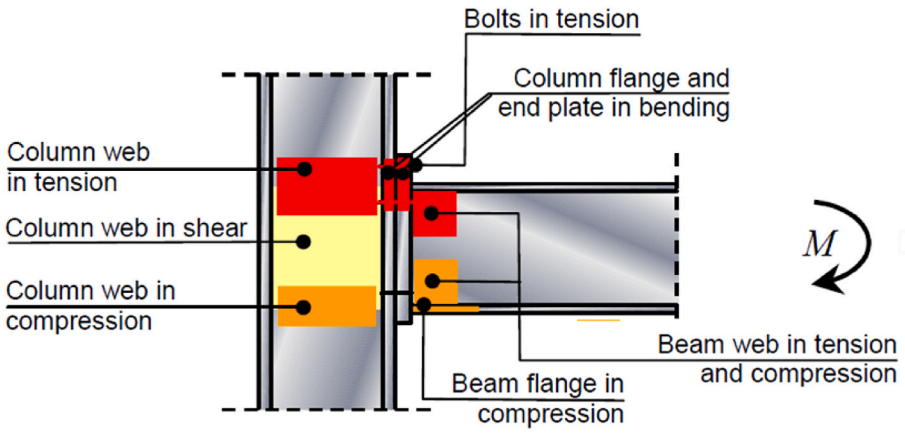

Fig. 8. Components of a beam-to-column joint according to EN 1993-1-8, [23].

- *beam flange and web in compression,*
- *column web in compression (or stiffener compression resistance),*
- *web panel in shear.*

Fifteen typical joint configurations are investigated in the first research program, 5 typical joints with 3 web depths as shown in Fig. 9. Five bolt rows are applied on all the joints (4 on the tension side, one on the compression side). Joints are subjected to pure bending moment according to the aim of the investigation. For each joint configurations one component is set to be weaker as the others to investigate the effect of partial stiffener on the resistance of the studied component. The identification of the weakest component was important in this study, which load carrying capacity governs the bending resistance of the joint.

It was also intended to select joint geometries representing the global structural behavior of typical joint configurations. The only component, which dimensions are not varied systematically in the parametric study is the stiffener thickness. The applied stiffener thickness is 12 mm (usual size in the praxis). The steel grade of the investigated joints is always

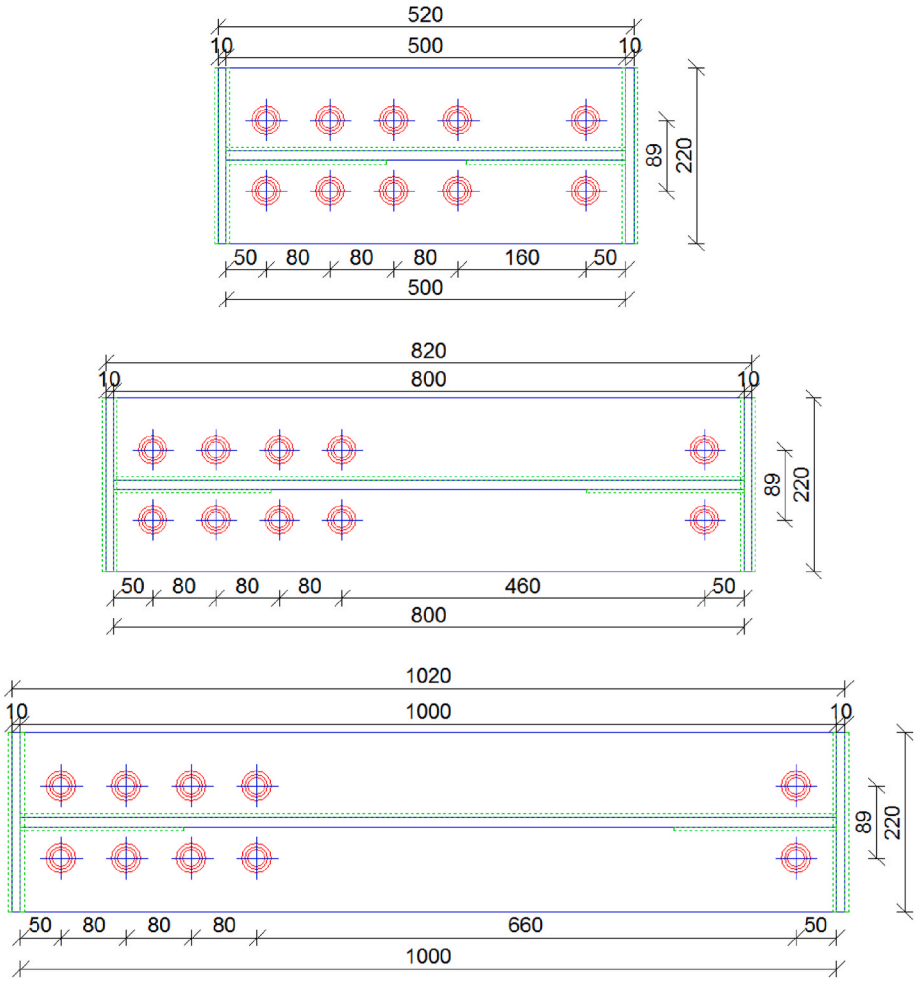

Fig. 9. General overview of the joints with 500 mm, 800 mm and 1000 mm web depth.

S355. Five bolt rows are applied in all the joints (4 on the tension side, one on the compression side). The applied bolts have a size and strength of M16 - M20 10.9 (d = 16–20 mm; f_{yb} = 900 MPa, f_{ub} = 1000 MPa). Each joint type is investigated with three different web depths (500–800 – 1000 mm) resulting in 15 joint configurations. For all the 15 joint configurations 4 numerical simulations are executed with different stiffener lengths. The joint (component) resistances with full length stiffener are considered as a reference value and three calculations are executed with stiffener lengths of 0,9–0,8–0,7·h_w, for all joint types. Therefore, a total of 60 numerical simulations are carried out to investigate the effect of partial stiffener. The calculated bending resistances of the joints with partial stiffeners are compared to the reference values (full length stiffener) and the influence of the partial stiffener on the component resistance has been analyzed.

The numerical calculations showed, the stiffener length (full or partial) has no influence on the tension side component resistances or if the flange and web in compression is the governing component. The numerical results are also compared in terms of bolt row force distribution and bending resistances. The results proved, there is no difference in the bolt row force distribution and bending resistance comparing the joint behavior with full and partial stiffeners, if the ultimate components are the followings:

- T-stub resistance (mode 1–2),
- T-stub resistance (mode 3),
- beam web in tension,
- flange and web in compression.

The only decrease in the bending resistance and changes in the bolt row forces was observed, if the ultimate component is the web panel in shear, which component is investigated more in a detailed manner within frame of a second numerical parametric study using the shell element model presented in the following Section. The comparison of the web panel stress distributions with full and partial stiffener can be seen in Fig. 10, which prove, that the stress distribution and the ultimate resistance changes as well, if partial stiffeners are used instead of full-length stiffeners.

4. Investigation of the web panel in shear resistance

4.1. Investigation strategy

The effect of partial stiffener on the web panel in shear resistance is investigated using models having four different web depths: 400, 500, 600 and 800 mm. For all web depths, different shear panel thicknesses are used to investigate different slenderness ratios (t_w = 3, 4, 5, 6 and 8 mm). Using these h_w/t_w ratios the relative slenderness of the investigated joints is varied between 0, 49 and 2,1. This slenderness range covers the usually used slenderness range in the design praxis and covers all the different parts of the web panel in shear resistance calculation method. Using these models, all the four components of the web panel in shear resistance could be investigated, which are the followings:

- plastic shear failure,
- buckling resistance of the web,
- tension band resistance,
- frame mechanism resistance.

All the simulations with different h_w/t_w ratios are carried out with small (150 × 12; 160 × 12; 200 × 12) and larger flanges (250 × 25; 300 × 25; 350 × 30) to be able to investigate the effect of the post-critical behavior of the tension band and frame mechanism. Within the numerical parametric study S355 steel grade has been applied with a yield and ultimate strength of f_y = 355 MPa and f_u = 510 MPa, respectively.

All these calculations are made on joints with full stiffener and with partial stiffener and the resistance reduction is determined by the comparison of these two values. Based on these, the effect of partial stiffener on the different components is evaluated and determined. Systematic additional calculations are also made for the design method development which aims are the investigation of the different components separately. For large slenderness ratios, where the ultimate component is the buckling resistance of the panel and the post-critical resistance of the tension band, an additional parametric study is made for slenderness ratios of 0,86, 1,08, 1,35 and 1,8.

To study the plastic shear failure mechanism of the web panel in shear resistance, panels with smaller slenderness ratios (0,49, 0,56 and 0,83) are also analyzed. The effect of the flange is studied systematically by using different flange width-to-thickness ratios and the effect of the frame mechanism is studied based on the numerical simulations. In the frame of the current numerical research program a total of 128 shear panel configurations are studied and 316 simulations are executed. The evaluation of the results is made separately for the plastic and for the buckling failure modes. In the current paper the main conclusions and the modified analytical model describing the failure mechanism of the shear panel resistance are presented.

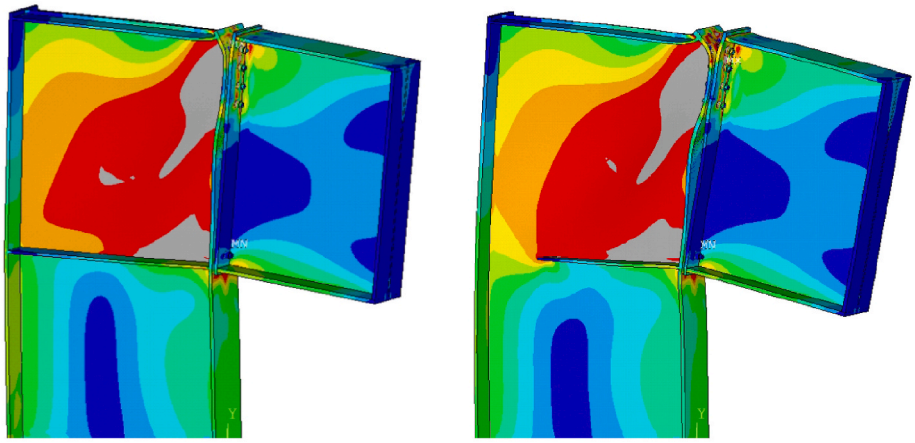

Fig. 10. Comparison of stress distribution diagrams.

4.2. Structural behavior: governing failure mode - plastic resistance of the web panel

If the relative slenderness of the investigated web panel is smaller than 0,83, the ultimate component which gives the lowest resistance is the plastic shear resistance. It might be determined by Eq. (1) according to EN 1993-1-8 [1].

$$V_{pl,R} = 0,9 \cdot \frac{Y \cdot t_w \cdot f_{y,w}}{\sqrt{3} \cdot \gamma_{M0} \cdot \beta} \tag{1}$$

where: Y is the web depth of the column,
t_w column web thickness,
$f_{y,w}$ yield strength of the column web,
β ratio of moments acting on opposite sides of the shear panel,
γ_{M0} partial factor.

The values of Y and t_w are varied within the current parametric study. The value of β is taken constant (β=1,00), thus only one-sided connections are investigated in the current study. One steel grade is investigated (S355) in the calculations and the partial safety factor in the comparison within the numerical simulations is set to 1,0. Based on the plastic shear resistance the total bending resistance of the shear panel may be determined by Eq. (2).

$$M_{w,R} = V_{pl,R} \cdot z + M_{FM,R} \tag{2}$$

where $M_{FM,R}$ is the moment resistance of the frame mechanism. The value of z is considered as the distance between the flange middle lines of the beam. The bolt position can have influence on the value of z, but in the current investigations the web panel in shear resistance is determined independently from the bolt row layout. In the first step of the evaluation process, for all the analyzed shear panel geometries the plastic shear resistance and the resistance of the frame mechanism are determined. The ratio of these two resistances is determined and presented in Fig. 11. The horizontal axis of the diagram shows the number of the investigated shear panel geometries, where the slenderness is smaller than 0,83. The red column shows the proportion of the plastic shear resistance, and the black part of the column represents the proportion of the frame mechanism. The results show in the case of the analyzed geometries the frame mechanism gives 10% of the shear panel resistance in average and its maximum value is 22%.

Then the ultimate failure mode of the analyzed joints with full and partial stiffeners are compared. The typical failure modes observed for web panels with small slenderness can be seen in Fig. 12 for full and partial stiffener joints, respectively.

Comparing the ultimate failure modes of the two joints, it can be observed, that in the case of the joint with full length stiffener all the four plastic hinges in the flanges can be clearly observed, and the structural behavior of the flange and the web panel is similar to the mechanical model used in the frame mechanism resistance determination method, as shown in Fig. 13a). In the case of joints with partial stiffener, the stiffener cannot provide with fix support the external flange of the column, what influences the location of the plastic hinge development in the flanges. Fig. 13b) presents the modified mechanical model of the frame mechanism for this specific case. The location of the plastic hinge at point O moves into the column shape and indicates smaller rotation angle than in the original one. Thus, the plastic hinges in the column flange have different locations, and the distance between the two hinges are larger, the rotation of the flange will be smaller, and the inner potential energy of the flange will be also smaller resulting in decrease in the resistance of the frame mechanism.

This modified structural behavior indicates there are two plastic hinges, which have the same deformations as the plastic hinges in the original design method (points M and L), and there are two plastic hinges, where the rotation angle is smaller, therefore their effectiveness (resistance) will be reduced (points O and N). The comparison of the moment – rotation curves with full and partial stiffener and the values of the calculated resistances based on the original design method can be seen in Fig. 14 for one typical case.

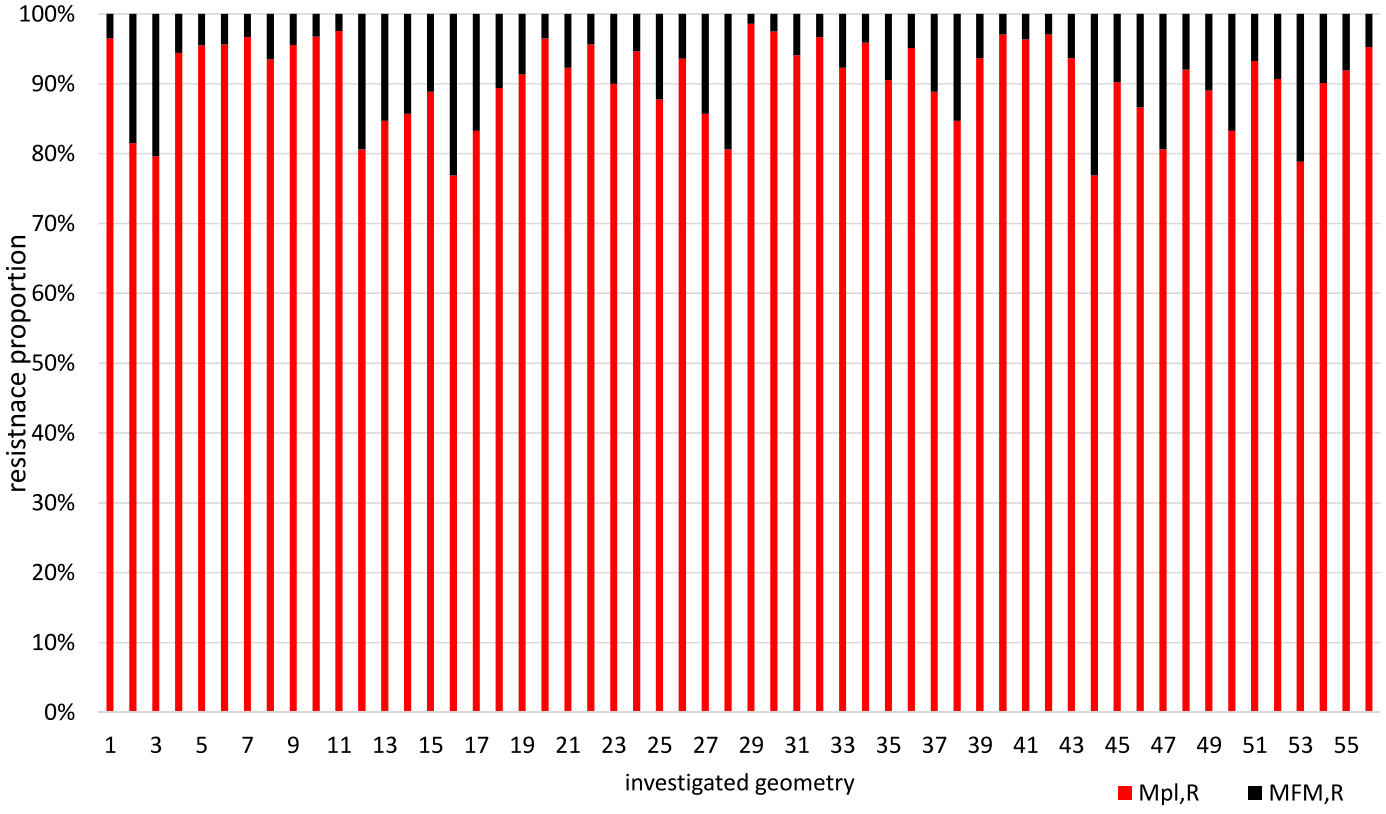

Fig. 11. Comparison of the plastic shear and frame mechanism resistances.

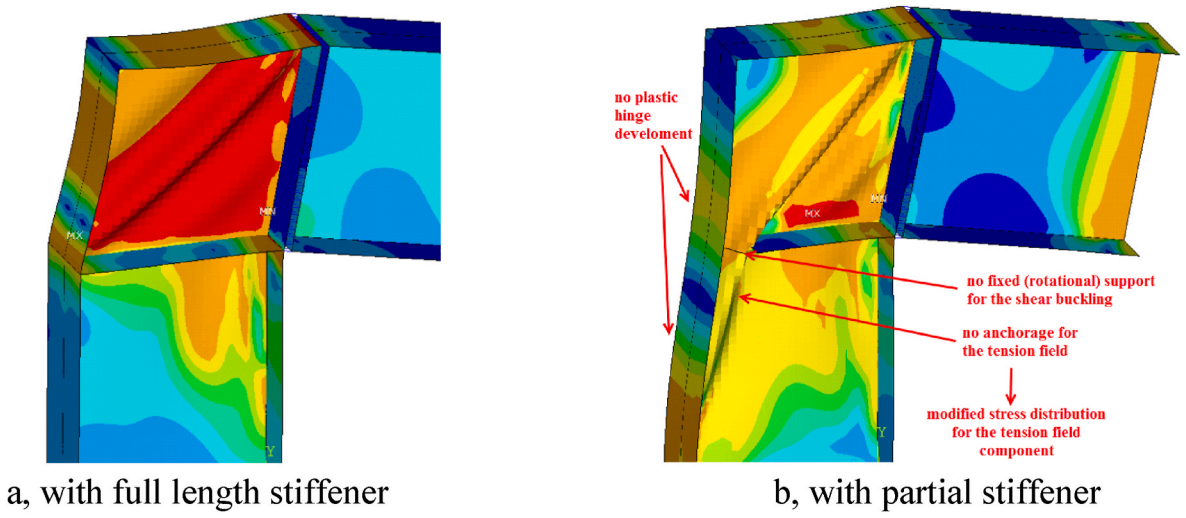

Fig. 12. Comparison of the observed failure modes.

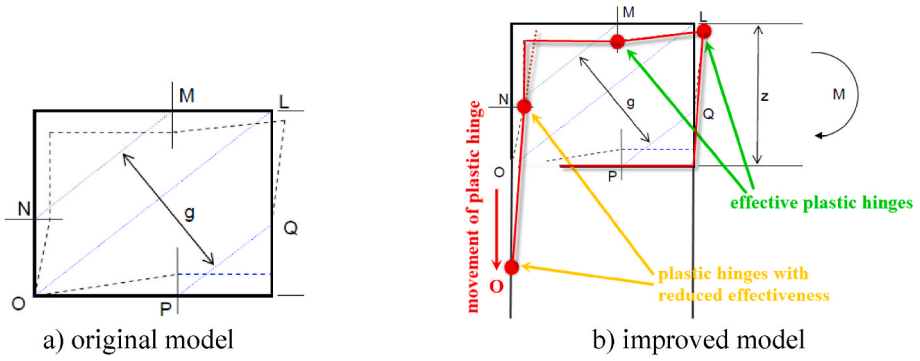

Fig. 13. Mechanical model of frame mechanism with a) full and b) partial stiffener.

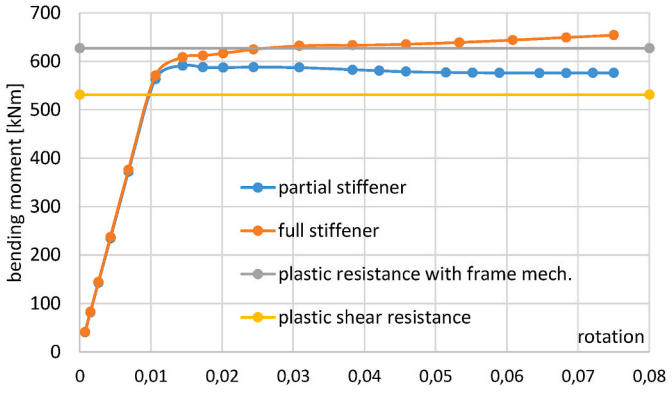

Fig. 14. Typical moment - rotation curves with full and partial stiffeners.

The diagram shows, the joint configuration with partial stiffener has larger resistances, than the plastic shear resistance of the joint. However, it is smaller than for joints with full stiffener or calculating using the original frame mechanism design model. On the other side, the joint with partial stiffener has smaller plastic reserve. Numerical calculations showed the entire frame mechanism cannot be considered in the shear panel resistance if partial stiffeners are applied. This observation is in full agreement with the observed failure mode and the modified mechanical model of the plastic failure mechanism. Based on the numerical parametric study, the plastic resistance of the frame mechanism can be reached by large deformations using full length stiffeners, but in the case of partial stiffeners the plastic reserve reduces. Therefore, consideration of the frame mechanism resistance in the design of moment transmitting joints is not recommended if partial stiffeners are applied.

It is important to highlight, the investigations with partial stiffener are related to partial stiffener length min. 70% of the column web depth. Shorter stiffeners were not investigated within the current parameter study; thus the stiffener is also required to eliminate another compression related failure modes of the joint. The column web in compression component of the EN 1993-1-8 component method is also a significant optional failure mode, which could be governing, if the stiffener would be significantly shorter, or if it would been eliminated. Therefore, to ensure join strength against column web in compression, the stiffener is necessary and cannot be eliminated. The above-described results are related to long, but not full-length stiffeners.

4.3. Structural behavior: governing failure mode – buckling of the web panel

If plate buckling governs the structural behavior – the total resistance of the web panel in shear can be determined by the sum of three different components, as shown in Fig. 2: (i) plate buckling V_{PB}, (ii) tension band V_{TB}, (iii) frame mechanism V_{FM}. The importance of these components is investigated and studied for the analyzed shear panel geometries, which characterize a wide application range of the shear panels used in the daily design. The comparison of the three components and its weight in the total web panel in shear resistance can be seen in Fig. 15. The weights of these components depend on the slenderness of the panel. In the case of very large slenderness ratios ($\lambda > 1{,}6$) the buckling resistance

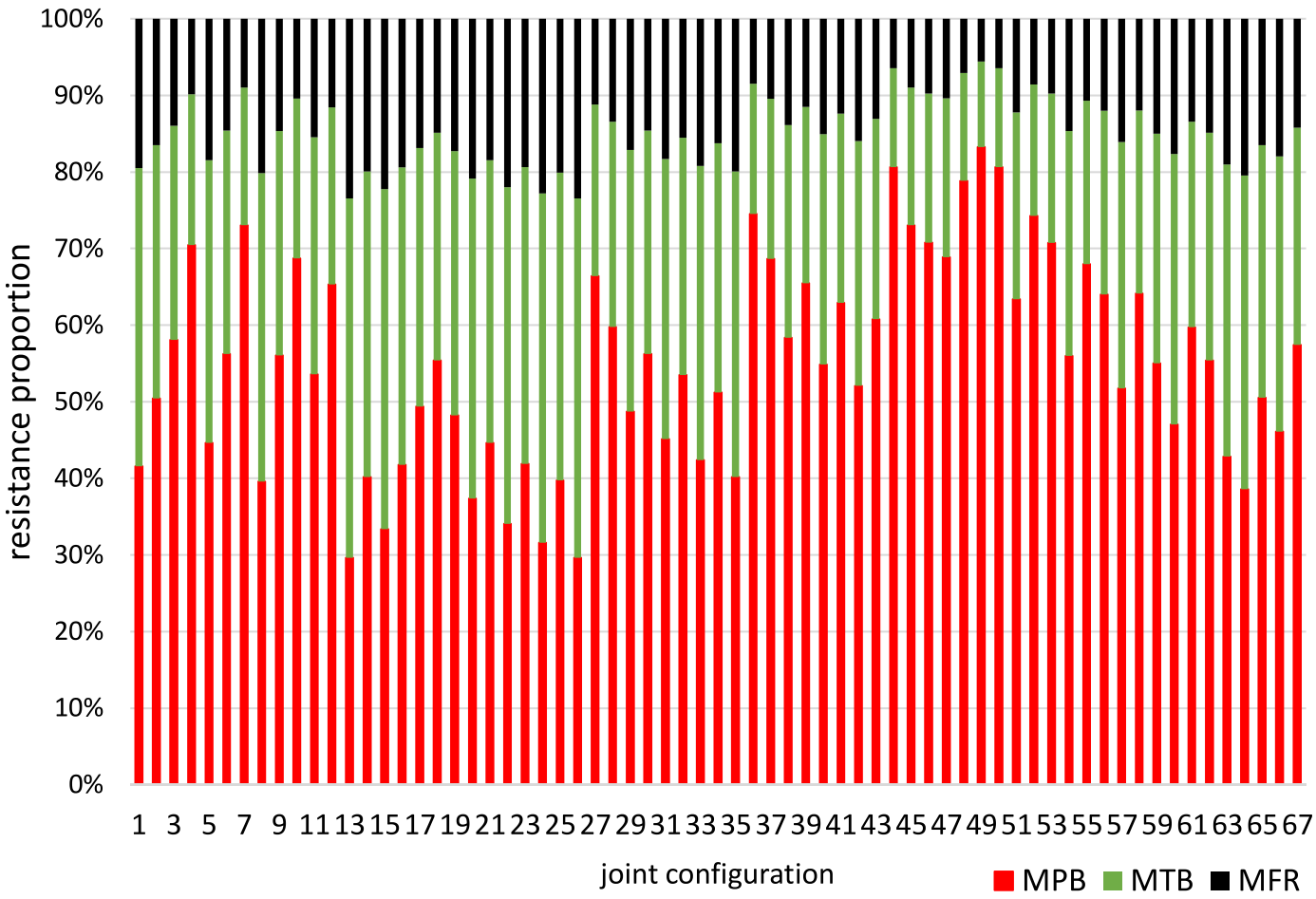

Fig. 15. Comparison of the resistance components.

and the tension band resistance are comparable (around 50-50%, or 40–60%) and each component has a large importance in the resistance. In the case of smaller slenderness ratios ($0{,}83 < \lambda < 1{,}6$), the buckling resistance of the web gives the dominant part (60–70%) of the web panel in shear resistance. The investigations also showed, frame mechanism component has the smallest part in the entire resistance. The structural behavior of the web panels with full and partial stiffener are compared and presented in Fig. 16 on a typical stress distribution diagram.

Based on the numerical simulations the following observations are made:

- there is no plastic hinge development in the column upper flange, the deformation field of the column flange is different for full and partial stiffener joints,
- the partial stiffener cannot give the same support condition to the web panel as the full stiffener against buckling, therefore the buckling behavior is slightly different,
- because the plastic hinge development in the column flange is different, the tension band cannot be anchored, and the tension band resistance decreases.

All these characteristics of the structural behavior should be

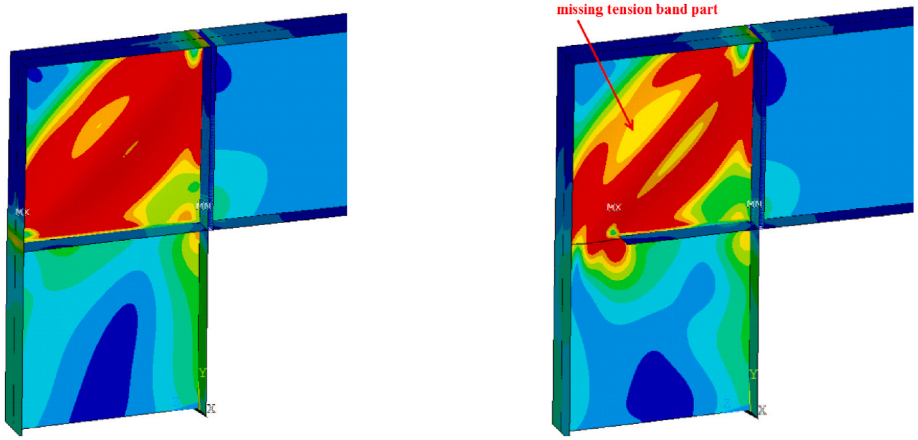

Fig. 16. Von Mises stress distributions a) with full and b) with partial length stiffener.

considered by the development of an enhanced design method. The modified structural behavior indicated the following necessary changes in the design model:

- frame mechanism component should be eliminated,
- buckling resistance should be modified due to the modified support conditions,
- tension band resistance should be modified due to reduced effectiveness, which comes from the anchorage difficulties at the free corner.

The typical stress distribution proving the mentioned above modified mechanism is shown in Fig. 17.

The buckling resistance can be determined according to EN1993-1-5 [15] based on the relative slenderness (λ_w) of the web. The slenderness ratio can be determined by Eq. (3):

$$\lambda_w = \sqrt{\frac{f_{y.w}}{\sqrt{3}\cdot\tau_{cr}}} \tag{3}$$

where: τ_{cr} is the elastic critical shear stress related to shear buckling of the web panel, calculated by Eq. (4):

$$\tau_{cr} = k_\tau \cdot \frac{\pi^2 \cdot E}{12\cdot(1-0.3)^2}\cdot\left(\frac{t_w}{Y}\right)^2 \tag{4}$$

k_τ is the buckling coefficient,

E is the Young's modulus of the steel material.

The current numerical simulations showed the stiffener and the column flange cannot provide with fixed support conditions to the web panel at the free corner if partial stiffeners are applied. Therefore, the buckling resistance can be approximated using a mechanical model with pinned support conditions and the buckling factor can be determined by Eq. (5).

$$k_\tau = \left(if\cdot a_r \geq 1;^{\circ}5.34 + \frac{4.0}{a_r{}^2};^{\circ}4.0 + \frac{5.34}{a_r{}^2}\right) \tag{5}$$

The tension band resistance depends on the (i) normal stresses acting in the web, (ii) width of the tension band and (iii) distance between the middle line of the tension band and the frame corner, as shown in Fig. 18. The tension band resistance can be calculated based on Eq. (6) if full length stiffeners are applied.

$$M_{TB} = \frac{\sigma_{TB}\cdot g\cdot t_w\cdot d}{\gamma_{M0}\cdot\beta} \tag{6}$$

where: σ_{TB} is the normal stress within the tension band, g and d are geometric measures as shown in Fig. 13 characterizing the width and location of the tension band.

If partial stiffeners are used in the joint, the tension band part between points ONML has a smaller effectiveness (as presented in Fig. 17),

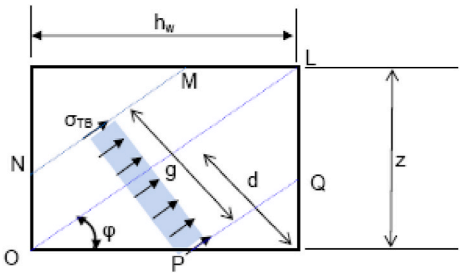

Fig. 18. Original mechanical model of tension band with full stiffener [21].

because the tension field cannot be anchored in the column flange. Therefore, only the tension bandwidth between points OP and LQ should be considered with its full value and the remaining part should be reduced to its 20%. It means that in the enhanced design method the tension bandwidth could be modified by replacing Eq. (7) by Eq. (8).

$$g = (ON + LQ)\cos(\alpha) \tag{7}$$

$$g = (ON\cdot 0,2 + LQ)\cos(\alpha) \tag{8}$$

All the other terms can be calculated by the same way as proposed in the international literature and developed by the original web panel is shear failure mechanism according to Ref. [4].

All the results of the numerical simulations are compared to the original design method (considering full tension band and frame mechanism) and to the enhanced design method. results are shown in Fig. 19.

Considering the results of the enhanced design method a good agreement can be observed between the numerical calculations and the analytical design method. The statistical evaluation of the two comparisons is also executed and presented in Table 3. The comparison validates the enhanced design method instead of the original one, what would lead to unsafe design in case of all the investigated shear panel geometries. The average overestimation would be 39% with large standard deviation (0,2). Using the enhanced design method, the average ratio between the results of the numerical simulations and the analytical design method is 95% with a standard deviation of 5%. The statistical evaluation shows, the enhanced design method is mainly on the safe side, it can be used for joints with partial stiffeners up to the stiffener length of 70% of the beam/column web depth.

4.4. Investigation of L-type joints with positive bending moment

All the previous investigations assumed, that the partial stiffener is placed on the compression side of the joint. The currently developed and presented enhanced design method is applicable only if the partial stiffener is placed on the compression side of the joint. The effect of the

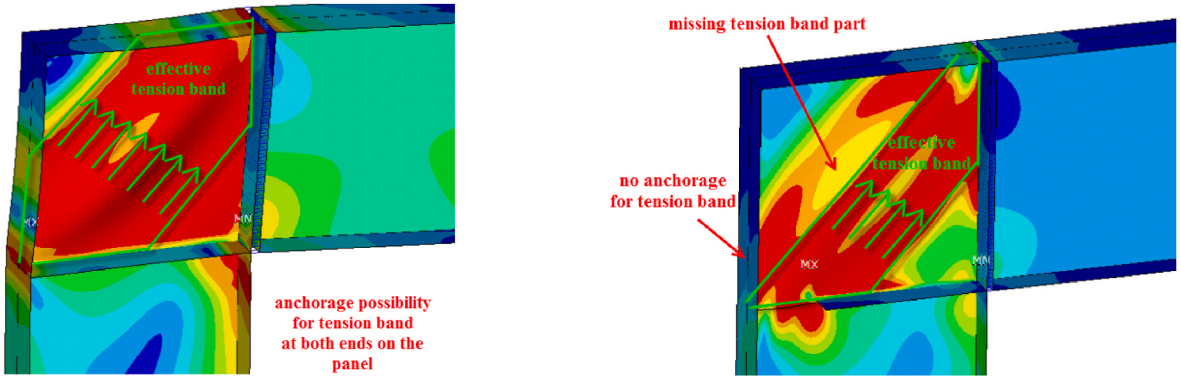

Fig. 17. Original tension band behavior with a) full and b) partial stiffener.

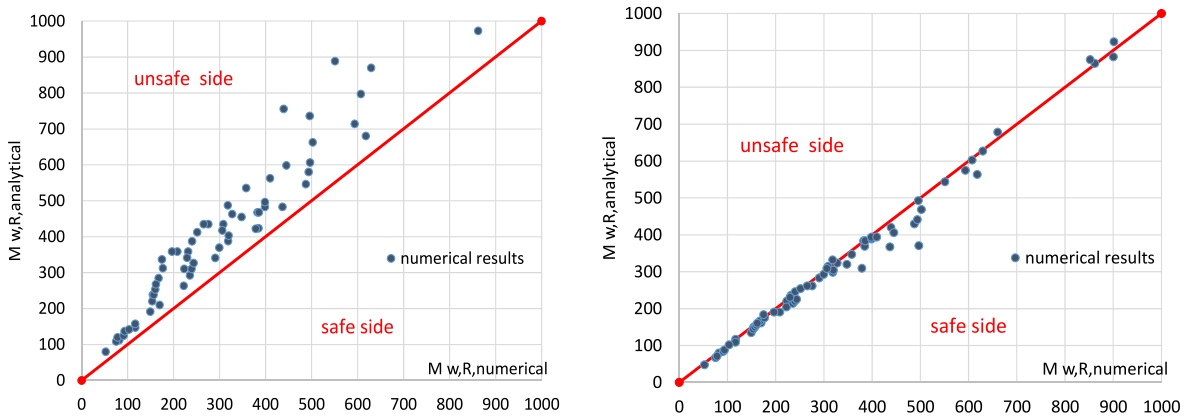

Fig. 19. Comparison of the numerical results with the a) original and b) improved design method.

Table 3
Statistical evaluation of the different design methods.

	original design method	enhanced design method
average ratio	1.39	0.95
standard deviation	0.20	0.05

partial stiffener on the joint structural behavior is also investigated if the partial stiffener is placed on the tension side of the joint, or the bending moment direction is changed (positive bending moment for beam-to-column joints). It must be mentioned that only one stiffener is created with partial stiffeners, the end plate of the joint is modeled as a full-length plate.

The comparison of the first eigenmode shape and the failure mode (as shown in Fig. 20) of a typical joint proves there is no large difference in the structural behavior and in the buckling resistance, if the partial stiffener is placed on the tension side.

The investigation of the stress distribution within the web panel and in the flanges prove that the partial stiffener has a negligible influence of the structural behavior of the joint. The plastic hinges in the flanges are not influenced by the partial stiffener, thus all the hinges are developing in the plates with full length (in the column upper flange and in the end plate of the joint). Therefore, the resistance of the frame mechanism and the tension band components are also not reduced by the application of the partial stiffener. The same result could be observed on the calculated moment-rotation curves as well.

The results of the current investigation prove that in case of load case combinations where the partial stiffener is located on the tension side, no modification of the original web panel in shear resistance calculation method is needed.

5. Effect of residual stresses on the structural behavior and resistance

5.1. Simplified numerical model for residual stresses analysis

In general, welded structures in civil engineering have large dimensional differences in length and height or width. A complex three-dimensional (3D) welding model need a large number of finite elements in the numerical simulation, to meet the computational accuracy of the high stress gradient in the region around the weld seams. However, 3D welding simulation need to consume a lot of computational resources and thus it is difficult to apply for structural design in practice. The most welded structural components in steel structures have the same cross-section in the length direction, such as welded beam and the welded steel element knee joints are essentially complex components with multiple welds. Theoretically, it is possible to use a simplified 2D welding simulation to simulate 3D welded components. And the obtained results in 2D model can be remodeled in a 3D model for mechanical calculation using the mapping method. The two important steps according to this approach are obtaining equivalent accuracy longitudinal residual stresses and strain from a 2D model and inputting the residual stresses or strains from the processed 2D cross-sections into 3D mode with a coarse mesh using some mapping algorithm.

The simplified procedure is related to the proposed local-global model developed by Launert [16], and Li et al. [17], which enables to implement the simplified 2D welding simulation. The scheme of the developed approach for residual stresses and bearing capacity analysis is displayed in Fig. 21. This approach mainly consists of strains, mapping relation algorithm to transfer obtained results as mechanical loads to a global model. Since high stress gradients in welded components are located in the weld seam, 2D welding simulation can focus computational resources on a representative partial area of the overall structure

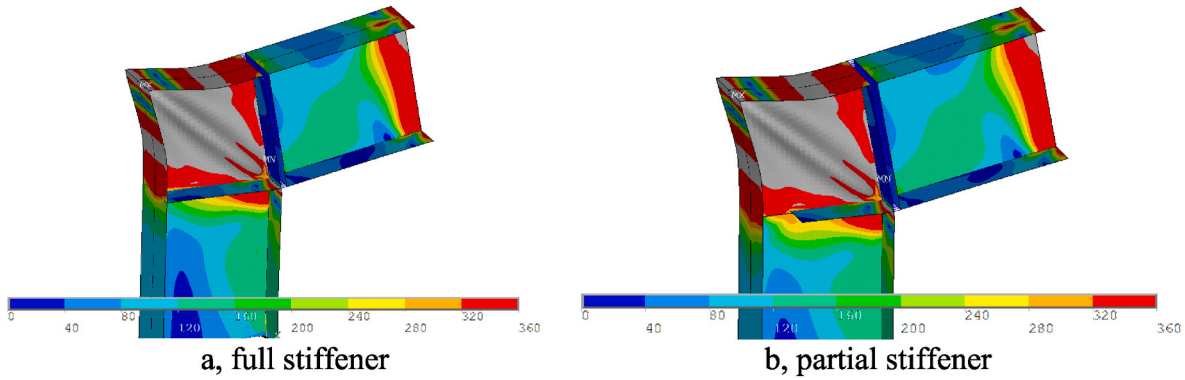

Fig. 20. Calculated typical failure modes.

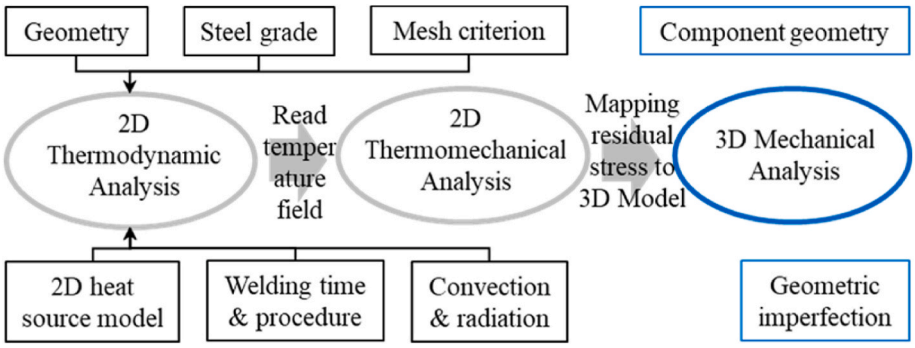

Fig. 21. Implemented scheme for the simplified calculation of weld residual stresses.

instead of the entire structural component, so that the calculation results can be quickly obtained. With this proposed approach, the partial area represents a 2D cross-sectional model and the corresponding computational times can in this way be kept very short. Usually, a 3D model of the entire components contains fewer elements and integration points in cross-sections compared to 2D model. Larger errors will produce, especially for thicker plates, if the 2D residual stress or strain results are directly mapped to the 3D whole structural component model, because fewer integration points will discard part of the result information. Therefore, the so-called sub-block model is developed as shown in Fig. 22. The basic idea of sub-block model is to simplify the welding plastic strain in the welded beam cross-section by one or more sub-block layers that can be defined easier using much coarser mesh. In general, this simplified numerical model for residual stress analysis can be divided into three steps:

Step 1. 2D thermomechanical welding simulation to calculate the plastic strains.

Step 2. Derivation of equivalent values or a sub-block strain model.

Step 3. Elastic FE analysis on the 3-D model with initial strains.

In this approach, residual inelastic strain is used as a link between the local and global models. On the one hand, this is because the inelastic strain can be easily replaced by thermal strain in the entire model. On the other hand, the distribution of residual strain on the cross-section is irrelevant to the size of the selected local model, namely partial cross-section, when the partial cross-section has sufficient stiffness. However, the distribution of residual stress is completely dependent on the size of the local model, as shown in Fig. 23. It is obvious the inelastic strains are generally limited to a very small area near the weld compared to the cross-section.

Because the inputs are time-consuming, a fully automatic execution of scripting software is efficient and necessary. Currently, the plugin LSH Welding Studio [16] based on ABAQUS® [18], which is a user interface program developed based on this simplified method, can provide efficient welding simulation and bearing capacity calculations for welded structural component with different cross-section.

5.2. *Numerical study on residual stress influence*

In this paper, a total of three specimens with different web thickness (6 mm, 8 mm and 10 mm) were simulated with the developed 2D simplified model, and the corresponding ultimate bearing capacity is calculated based on GMNIA. All steel plate junctions are joined using fillet weld of 4.5 mm. The mechanical material properties are defined depend on temperature according to Refs. [19,20] and the welding speed and energy including current, voltage, etc. are obtained according to the formula suggested in Ref. [16]. For the 2D welding simulation, the convection and diffusion quadrilateral element DCC2D4 with thermal conduction capability is employed and the shell element S4R and S3 are used for calculating the bearing capacity of welded steel element knee joint with partial height (70% and 90%) web stiffeners. This simplified 2D welding simulation is very efficient and just need limited calculation time comparing the traditional 3D welding simulation. Totally, the heat transfer analysis and thermomechanical analysis take just about half an hour.

Fig. 24 shows the results of the numerical simulation considering and ignoring residual stresses induced by the welding process. It is clearly according to Fig. 24a) that the knee joint mainly contains residual stresses before the loading process and the shear stress on the web increases and becomes the dominant component, as the loading progresses This phenomenon is shown in Fig. 24a) for four different displacement (loading) levels. The sketch belonging to zero displacement presents the pure welding induced residual stress distribution. Further sketches show the development of the stresses within the joint by increasing the load until the failure and large plastic deformations are reached.

In general, the residual stress caused by welding does not have a great influence on the bearing capacity of the welded steel element knee

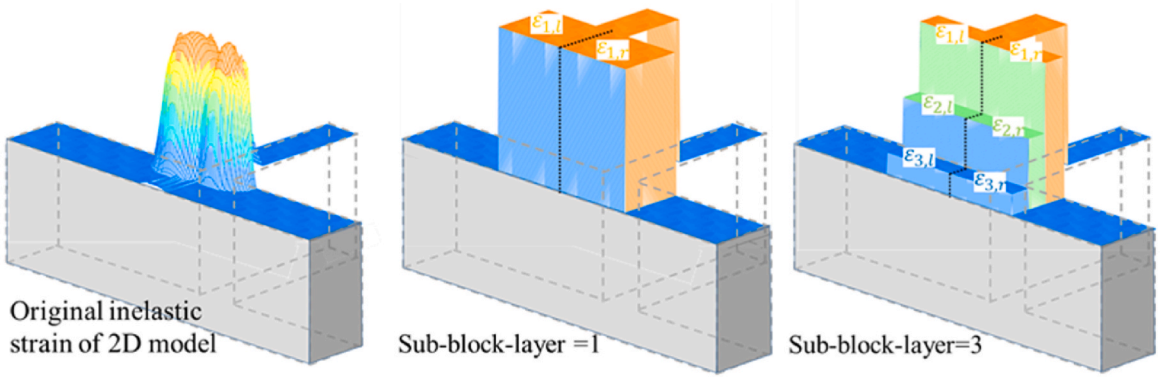

Fig. 22. Schematic representation of sub-block model.

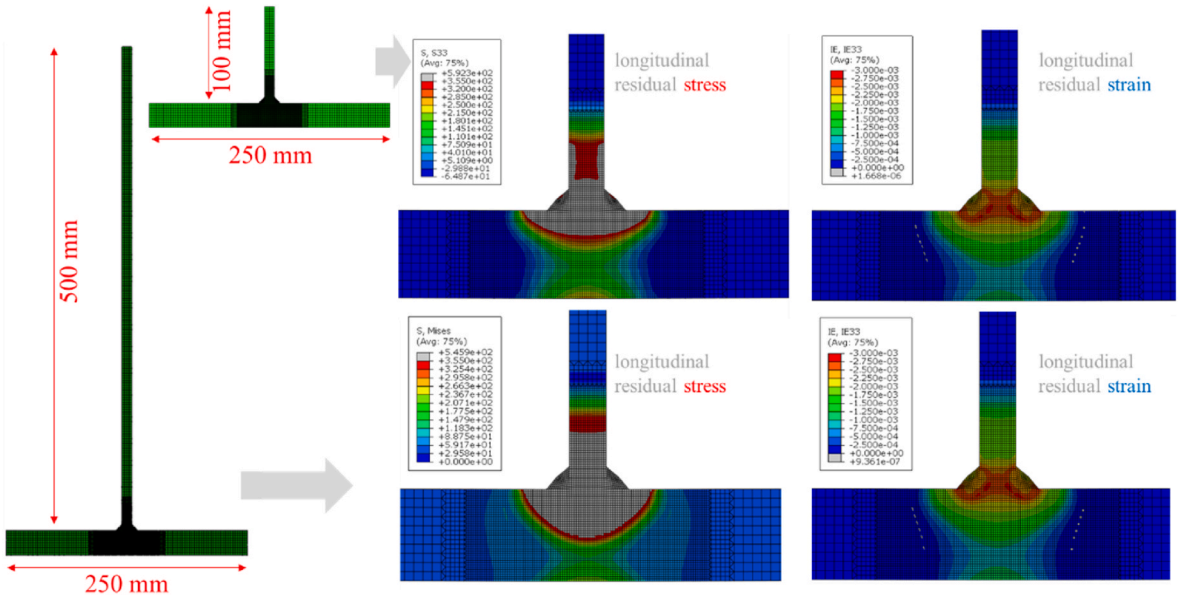

Fig. 23. Comparison of residual stresses and strains in different local sections.

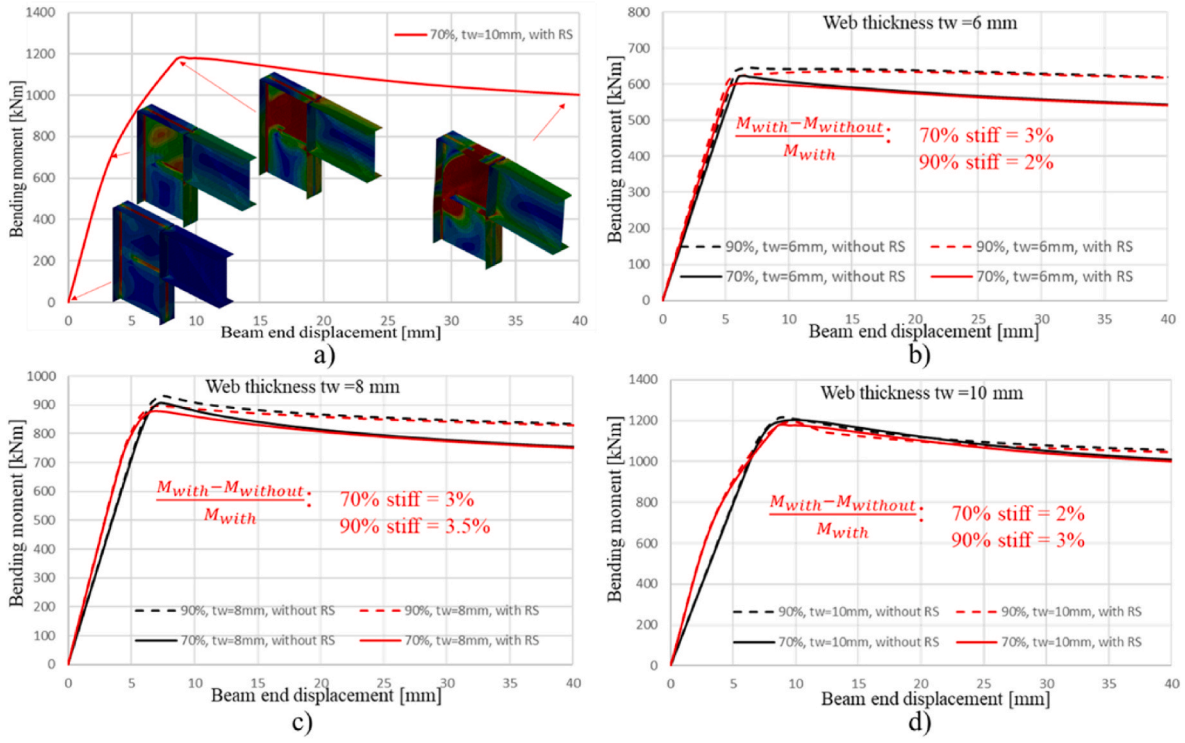

Fig. 24. Bending moment versus beam end displacement of welded knee joint, a) stress distribution by different phase, b) 6 mm web plate, c) 8 mm web plate, d) 10 mm web plate.

joints with partial height web stiffeners, which has the risk of web buckling stability problem. According to Fig. 19, the difference of bending capacity of the knee joints with and without consideration of residual stress is just about 3%. This may be due to the fact that the residual stress is balanced in the section perpendicular to the weld, in other words, the residual tensile and compressive stresses are canceling each other out. It can be interpreted that the dominant region of shear buckling lies on the diagonal of web, but the peak of residual stress is always at the weld at the edge of the web. Additionally, it can be observed on the moment-deflection diagrams, the welding-induced residual stress will result in earlier first yielding at a lower load level, than without modeling the residual stresses. This could have effect only on the first yielding limit state criteria. But beam-to-column joints are usually designed based on plastic resistance, therefore, the first yielding limit state does not limit the design resistance of the structure. However, the effect of the residual stresses can be clearly seen on the calculation results, which increases by increasing web thickness.

6. Conclusion

The impact of a partial stiffener on the joint components according EN1993-1-8 and the Astron Buildings ETA-18/1027 can be summarized as follows for the case when the partial stiffener is located on the compression side of the joint, i.e. when the knee is under negative bending moment:

a. A negligible influence was observed on the tension side components of the bolted connection and the flange and web in compression component. No change of failure mode was observed when one of these components is critical.
b. A major influence was observed on the web panel in shear components with effect on the failure mode, on the bolt forces distribution and subsequently on the bending moment resistance. Therefore, the parametric study has focused on the web panel in shear resistance and on the effect of the partial stiffeners on its resistance.

The comparison of full stiffener and partial stiffener cases has allowed to identify how the web panel slenderness and the size of the gap influence the components. Modified calculation methods were elaborated, which were presented in the paper in a detailed manner. Its summary is as follows:

a. Shear buckling failure V_{PB}: the free corner at the gap cannot provide the usual rigid support for the web panel. Pinned support conditions shall be applied at the free corner resulting into a reduced critical shear stress value.
b. Post-critical tension failure V_{TB}: the gap does not allow to anchor the tension band as usual and a reduced tension band width must be considered. A larger gap means a higher reduction of the band width and subsequent reduction of the component resistance.
c. Plastic failure: the frame mechanism V_{FM} is modified by the presence of the gap. The location of the plastic hinges is changing, and the mechanism takes a modified shape. This is considered by providing adjusted resistance calculation formulations depending on the web slenderness.
d. All other components of the joint may be calculated the same way as for the case with full-size stiffener. When the partial stiffener is on the tension side of the knee joint, i.e. knee under positive bending moment, no influence on the knee resistance could be identified.

The novel modeling technique has been presented in the paper on the application of welding residual stresses and imperfections by using welding simulation technique. The advantages and the impact of the welding induced imperfections are presented and discussed in the paper. The main conclusion of the study were the followings:

a. the proposed simplified modeling technique leads to accurate shear buckling resistance of the modeled joints and well-applicable for complex structural details,
b. Calculations also prove, the welding-induced residual stresses and imperfections have similar effects than the equivalent geometric imperfections. The largest difference between the two calculation results were only 3%, which fits to the expectations on a failure mode having large plastic reserve and post-critical buckling behavior.

Declaration of competing interest

The authors declare that they have no known competing financial interests or personal relationships that could have appeared to influence the work reported in this paper.

Data availability

No data was used for the research described in the article.

Acknowledgement

The preparation of the paper has been financially supported by the Grant MTA-BME Lendület LP2021-06/2021 “Theory of new generation steel bridges” program of the Hungarian Academy of Sciences, which is gratefully acknowledged.

References

[1] EN 1993-1-8:2005; Eurocode 3: Design of steel structures, Part 1-8: Design of joints, 2005.
[2] ETA-18/1027 “Astron Building System”, DIBt.
[3] J. Scheer, H. Pasternak, T. Schween, On the structural behavior of stiffened knee joints with thin webs, ASCE J. Structural Division 117 (1991) 2600–2619.
[4] I. Vayas, H. Pasternak, T. Schween, Beanspruchbarkeit und Verformung von Rahmenecken mit schlanken Stegen, Bauingenieur 69 (1994) 311–317.
[5] I. Vayas, J. Ermopoulos, H. Pasternak, Design of steel frames with slender joint-panels, J. Constructional Steel Res. 35 (1995) I65–I187.
[6] L. Dunai, B. Kövesdi, Application Possibility of Partial Stiffeners in Beam-To-Column Joints, Expert report for Astron Buildings s.a., 2014 extended in (2015.
[7] ANSYS® v17.1, Canonsburg, Pennsylvania, USA.
[8] B. Kövesdi, L. Dunai, Shear Panel Reinforcement Design, Research Report, BME Department of Structural Engineering, Budapest University of Technology and Economics, 2012.
[9] J. Lemaitre, J. Dufailly, Damage measurements, Eng. Fract. Mech. 28 (1987) 643–661.
[10] N. Bonora, D. Gentile, A. Pirondi, G. Newaz, Ductile damage evolution under triaxial state of stress: theory and experiments, Int. J. Plast. 21 (2005) 981–1007.
[11] M. Brünig, M. Alves, Experiments and numerical analysis of anisotropically damaged elastic–plastic solids, in: D.R.J. Owen, E. Onate, B. Suárez (Eds.), Computational Plasticity VIII, CIMNE, Barcelona, 2005, pp. 873–876.
[12] D.J. Celentano, J.L. Chaboche, Experimental and numerical characterization of damage evolution in steels, Int. J. Plast. 23 (2007) 1739–1762.
[13] L. Dunai, B. Kövesdi, Bolt-row Force Distribution in the Hammerhead, Expert Report, BME Department of Structural Engineering, 2013.
[14] L. Katula, Computer Based Analysis of Frames Considering Semi-rigid Joint Behaviour, Diploma Thesis, BME Department of Steel Structures, Technical University of Budapest, 1993.
[15] EN1993-1-5:2005; Eurocode 3: Design of Steel Structures, Part 1-5, Plated structural elements, 2005.
[16] B. Launert, Untersuchungen an geschweißten I-Trägern aus normal- und hochfestem Baustahl: Beitrag zur Erweiterung der Tragfähigkeitsnachweise durch Einsatz der Schweißsimulation (Dissertation), Schriftenreihe Stahlbau, BTU, Cottbus, 2019.
[17] Z. Li, H. Pasternak, J. Wang, T. Krausche, B. Launert, Bending Capacity of Single and Double Sided Welded I-Sectional Girders: Part 2 - Simplified Welding Simulation and Buckling Analysis, Proceedings of the Eighth International Conference on Structural Engineering, Mechanics and Computation, SEMC 2022), Cape Town, 2022.
[18] ABAQUS/Standard User’s Manual, Version 6.9, Michael Smith, 2009.
[19] U. Peil, M. Wichers, Schweißen unter Betriebsbeanspruchung - werkstoffkennwerte für einen S355 J2G3 unter Temperaturen bis 1200°C, Stahlbau 73 (2014) 400–416.
[20] O. Voß, Untersuchung relevanter Einflussgrößen auf die numerische Schweißsimulation (Dissertation), Shaker Verlag, Aachen, 2001.
[21] J.P. Jaspart, Expert Report on Particular Aspects of the Design Verification of Astron Light Gage Steel Building Bolted Moment Connections, University of Liège, ArGEnCo Department, 2010.
[22] L. Katula, Bolted End-Plate Joints for Crane Backets and Beam-To-Beam Connections, PhD dissertation, Department of Structural Engineering, Budapest University of Technology and Economics, 2007.
[23] F.M. Block, I.W. Burgess, J.B. Davison, Numerical and Analytical Studies of Joint Component Behaviour in Fire, Third International Workshop <<Structures in Fire>>, Ottawa, 2004, p. 12.